Mon. Not. R. Astron. Soc. **348,** 625–637 (2004) doi:10.1111/j.1365-2966.2004.07399.x

Inertial modes of non-stratified superfluid neutron stars

R. Prix,[1⋆†] G. L. Comer[2] and N. Andersson[1]
[1]*Department of Mathematics, University of Southampton, Southampton SO17 1BJ*
[2]*Department of Physics, Saint Louis University, St Louis, MO 63156, USA*

Accepted 2003 November 4. Received 2003 October 23; in original form 2003 August 22

ABSTRACT

We present results concerning adiabatic inertial-mode oscillations of non-stratified superfluid neutron stars in Newtonian gravity, using the anelastic and slow-rotation approximations. We consider a simple two-fluid model of a superfluid neutron star, where one fluid consists of the superfluid neutrons and the second fluid contains all the comoving constituents (protons, electrons). The two fluids are assumed to be 'free' in the sense that vortex-mediated forces such as mutual friction or pinning are absent, but they can be coupled by the equation of state, in particular by entrainment. The stationary background consists of the two fluids rotating uniformly around the same axis with potentially different rotation rates. We study the special cases of corotating backgrounds, vanishing entrainment, and the purely toroidal r modes analytically. We calculate numerically the eigenfunctions and frequencies of inertial modes in the general case of non-corotating backgrounds, and study their dependence on the relative rotation rate and entrainment. In these non-stratified models, we find avoided crossings only between associated mode pairs, e.g. an 'ordinary' mode and its 'superfluid' counterpart, while other mode frequencies generally cross as the background parameters are varied. We confirm (for the first time in a mode calculation) the onset of a 'two-stream instability' at a critical relative background rotation rate, and we study some of the properties of this instability for the inertial modes.

Key words: dense matter – hydrodynamics – instabilities – stars: neutron – stars: oscillations – stars: rotation.

1 INTRODUCTION

The oscillations of rotating compact stars are a subject that has attracted interest for a considerable time. This is natural because the associated issues range from fundamental applied mathematics (e.g. the stability of rotating self-gravitating fluid configurations), to mainstream astrophysics (e.g. helioseismology and attempts to infer the Sun's rotation profile from observed modes of oscillation) and exotic neutron-star physics (e.g. the gravitational-wave driven instability of the r modes and various viscous damping mechanisms, such as hyperon bulk viscosity). To date, most investigations have assumed that a rotating star can be appropriately described by a perfect fluid model. While such models are relevant in many contexts, they do not provide an adequate description of mature neutron stars. Once a neutron star has cooled below 10^9–10^{10} K, i.e. within minutes to months after its birth, its outer layers will form a crystalline lattice of nuclei. At the same time, the fluid core is expected to contain several superfluid/superconducting components.

This paper concerns the dynamics of rotating superfluid neutron stars. In particular, we study the inertial modes of a simple two-fluid model appropriate for the conditions that prevail in the outer core of a neutron star. The two fluids, which represent superfluid neutrons and a conglomerate of all comoving constituents (protons, electrons), are coupled via the equation of state (in particular via entrainment), but are otherwise allowed to move at independent velocities. Our background model is a stationary two-fluid configuration with constant entrainment, with the two fluids rotating uniformly around the same axis with rotation rates Ω_n and Ω_p.

Previous studies of superfluid inertial modes (including preliminary studies of the zero-frequency subspace), namely Lindblom & Mendell (2000), Sedrakian & Wasserman (2000), Andersson & Comer (2001), Comer (2002), Lee & Yoshida (2003) and Yoshida & Lee (2003a,b), have all been restricted to corotating backgrounds $\Omega_n = \Omega_p$. This study is the first to allow for the general case of a background with two fluids rotating at different rates. This is expected to be the quasi-stationary 'ground state' of a superfluid neutron star due to its emission-induced spin-down and the weak coupling to the superfluid components. This background model is also the starting point of all viable models of Vela-sized glitches. In other words, by allowing for different rates of rotation, we have taken a crucial step towards more realistic modelling of the dynamics of mature neutron stars.

⋆Present address: Albert-Einstein Institut, Am Mühlenberg, 14476 Golm b. Potsdam, Germany.
†E-mail: Reinhard.Prix@aei.mpg.de

2 THE TWO-FLUID NEUTRON-STAR MODEL

We take as our starting point the 'standard' two-fluid model for superfluid neutron stars (e.g. Lindblom & Mendell 1994; Lee 1995; Langlois, Sedrakian & Carter 1998; Prix & Rieutord 2002; Prix 2003a), in which we assume that the protons and electrons are locked together by the magnetic field and viscosity, while the superfluid neutrons form an independent fluid due to their lack of viscosity. Our model neglects the presence of the elastic crust as well as the potential presence of exotic matter in the deep neutron-star core. In essence, the model is expected to be relevant for the outer neutron-star core. By studying the global modes of oscillation of this model, we hope to gain insight into the complex dynamics of any two-fluid system. Even though we are not considering a detailed realistic neutron-star model (the construction of which would be very difficult given our current level of understanding) we expect to learn much about qualitative aspects that should remain relevant also in more complicated settings. It is also interesting to note, cf. comments made by Sedrakian & Wasserman (2000), that the study of two-fluid models may be of significance in laboratory contexts, for example in the study of rotating heavy nuclei using the compressible liquid approximation of the Bohr–Wheeler model, or for rotating mixtures of Bose–Einstein condensates.

A general Newtonian formalism to describe mixtures of charged and uncharged fluids has been developed by Prix (2003a,b), based on a variational principle that was first developed in a fully relativistic framework by Carter and coworkers (Carter 1989; Carter & Khalatnikov 1992; Carter & Langlois 1998). In particular, Prix (2003a) developed a general two-fluid neutron-star model allowing for temperature gradients and dissipation through mutual friction and β-reactions between the two fluids. For the present application, however, we assume a 'cold' neutron star in which we can neglect temperature effects, so we set $T = 0$, and we also neglect mutual friction and non-adiabatic processes such as β-reactions. The resulting framework, which is identical to that used by Prix & Rieutord (2002) and Andersson & Comer (2001), is briefly introduced in this section. Note that, although the formalism used here is different from that more commonly found in the Newtonian literature (Lindblom & Mendell 1994; Lee 1995; Lee & Yoshida 2003), which is based on the 'orthodox' superfluid formalism introduced by Landau, the two frameworks can be shown to be strictly equivalent, as discussed by Prix (2003a).

Our two-fluid model consists of a neutron and a 'proton' fluid (the latter actually consists of the comoving protons and the electrons). Therefore, the kinematic variables are the particle number densities $n_{\rm n}$ and $n_{\rm p}$ together with the respective transport velocities $\boldsymbol{v}_{\rm n}$ and $\boldsymbol{v}_{\rm p}$. The corresponding transport currents are naturally expressed as

$$\boldsymbol{n}_X = n_X \boldsymbol{v}_X, \tag{1}$$

where $X \in \{\rm n, p\}$ is the constituent index (the repetition of which does not imply summation). An important quantity for our analysis is the relative velocity $\boldsymbol{\Delta}$ between the two fluids, which we define as

$$\boldsymbol{\Delta} \equiv \boldsymbol{v}_{\rm p} - \boldsymbol{v}_{\rm n}. \tag{2}$$

The dynamics is governed by the Lagrangian density

$$\Lambda = \frac{1}{2} n_{\rm n} m_{\rm n} \boldsymbol{v}_{\rm n}^2 + \frac{1}{2} n_{\rm p} m_{\rm p} \boldsymbol{v}_{\rm p}^2 - \mathcal{E} - \rho\Phi, \tag{3}$$

where $\rho \equiv m_{\rm n} n_{\rm n} + m_{\rm p} n_{\rm p}$ is the total mass density, Φ is the gravitational potential and $\mathcal{E}$ is the energy function or 'equation of state' of the system. The general form of the equation of state is $\mathcal{E} = \mathcal{E}(n_{\rm n}, n_{\rm p}, \boldsymbol{\Delta}^2)$, which determines the first law of thermodynamics in the form

$$\mathrm{d}\mathcal{E} = \mu^{\rm n}\mathrm{d}n_{\rm n} + \mu^{\rm p}\mathrm{d}n_{\rm p} + \alpha\mathrm{d}\boldsymbol{\Delta}^2, \tag{4}$$

defining the chemical potentials $\mu^{\rm n}$ and $\mu^{\rm p}$, as well as the entrainment α. The conjugate momenta for the two fluids are defined by the total differential of the Lagrangian density Λ, namely

$$\mathrm{d}\Lambda = \sum_{X={\rm n,p}} \left[\boldsymbol{p}^X \cdot \mathrm{d}\boldsymbol{n}_X + \left(p_0^X - m^X\Phi\right)\mathrm{d}n_X\right] - \rho\,\mathrm{d}\Phi, \tag{5}$$

In the following we assume the two masses to be equal, so we set $m^{\rm p} = m^{\rm n} = m_{\rm b}$. With the explicit form (3) of the Lagrangian and the first law (4), we can express these conjugate momenta as

$$\boldsymbol{p}^{\rm n} = m_{\rm b}(\boldsymbol{v}_{\rm n} + \varepsilon_{\rm n}\boldsymbol{\Delta}), \tag{6}$$

$$\boldsymbol{p}^{\rm p} = m_{\rm b}(\boldsymbol{v}_{\rm p} - \varepsilon_{\rm p}\boldsymbol{\Delta}), \tag{7}$$

$$p_0^{\rm n} = -\mu^{\rm n} + \frac{1}{2} m_{\rm b} \boldsymbol{v}_{\rm n}^2 - \boldsymbol{v}_{\rm n} \cdot \boldsymbol{p}^{\rm n}, \tag{8}$$

$$p_0^{\rm p} = -\mu^{\rm p} + \frac{1}{2} m_{\rm b} \boldsymbol{v}_{\rm p}^2 - \boldsymbol{v}_{\rm p} \cdot \boldsymbol{p}^{\rm p}, \tag{9}$$

where we have defined the dimensionless parameters ε_X characterizing entrainment by

$$\varepsilon_X \equiv \frac{2\alpha}{m_{\rm b} n_X}. \tag{10}$$

Sometimes it is more convenient to use a single entrainment parameter ε, which we choose to be $\varepsilon_{\rm p}$, so we have

$$\varepsilon_{\rm p} = \varepsilon, \qquad \text{and} \qquad \varepsilon_{\rm n} = \frac{x_{\rm p}}{1 - x_{\rm p}}\varepsilon, \tag{11}$$

in terms of the proton fraction $x_{\rm p}$, which is naturally defined as

$$x_{\rm p} \equiv \frac{n_{\rm p}}{n}, \qquad \text{with} \qquad n \equiv n_{\rm n} + n_{\rm p}. \tag{12}$$

We note that this definition of the entrainment ε is different from another definition, which we denote as ϵ, and which is sometimes found in the literature (e.g. Lindblom & Mendell 2000; Lee & Yoshida 2003). The relation between these two different definitions is simply (see Prix, Comer & Andersson 2002, for further discussion)

$$\epsilon = \frac{\varepsilon n_{\rm p}}{n_{\rm n} - \varepsilon n}. \tag{13}$$

We assume that the time-scale of oscillations is much shorter than that of β-reactions. Therefore, strict conservation of neutrons and protons applies, i.e. we have

$$\partial_t n_{\rm n} + \nabla \cdot (n_{\rm n}\boldsymbol{v}_{\rm n}) = 0, \tag{14}$$

$$\partial_t n_{\rm p} + \nabla \cdot (n_{\rm p}\boldsymbol{v}_{\rm p}) = 0. \tag{15}$$

As shown by Prix (2003a), the equations of motion for the two fluids can be derived from the Lagrangian density (2) using a 'convective' variational principle. They can be written in the form

$$(\partial_t + \boldsymbol{v}_X \cdot \nabla)\boldsymbol{p}^X + p_i^X \nabla v_X^i - \nabla Q^X = \frac{\boldsymbol{f}^X}{n_X}, \tag{16}$$

where $\boldsymbol{f}^X$ is the 'external' force density acting on the fluid X, and the scalars Q^X are defined as

$$\begin{aligned} Q^X &\equiv p_0^X - m^X\Phi + \boldsymbol{v}_X \cdot \boldsymbol{p}^X \\ &= -\mu^X + \tfrac{1}{2} m_{\rm b} \boldsymbol{v}_X^2 - m_{\rm n}\Phi. \end{aligned} \tag{17}$$

In the absence of 'external' forces acting on the whole system, the hydrodynamic force densities $\boldsymbol{f}^X$ in equation (16) have to satisfy $\boldsymbol{f}^{\rm n} + \boldsymbol{f}^{\rm p} = 0$ as a Noether identity of the variational principle. This still allows us to describe a mutual force $\boldsymbol{f}_{\rm mut}$ acting between the two fluids. It could be caused, for example, by collisions of the electrons with the neutron vortices (see, for example, Alpar, Langer & Sauls 1984). Such a model would be characterized by $\boldsymbol{f}^{\rm n} = -\boldsymbol{f}^{\rm p} = \boldsymbol{f}_{\rm mut}$. As a first step, however, we only consider the 'free' limit and postpone the inclusion of mutual friction and viscosity to future work. Our 'free' model is therefore characterized by

$$\boldsymbol{f}^X = 0, \qquad \text{for} \qquad X = \text{n, p}. \tag{18}$$

3 THE STATIONARY BACKGROUND

We assume the background to be stationary and axisymmetric, with both fluids rotating around the z-axis with rotation rates $\Omega_{\rm n}$ and $\Omega_{\rm p}$ respectively. Hence

$$\boldsymbol{v}_X = \Omega_X \boldsymbol{\varphi}, \qquad \text{and} \qquad \boldsymbol{\Delta} = (\Omega_{\rm p} - \Omega_{\rm n})\boldsymbol{\varphi}, \tag{19}$$

where $\boldsymbol{\varphi}$ is the axial Killing vector, given by

$$\boldsymbol{\varphi} = \frac{\partial x^i}{\partial \varphi}\partial_i = \partial_\varphi. \tag{20}$$

In spherical coordinates, i.e. $x^i \in \{r, \theta, \varphi\}$, this vector has the components $\varphi^i = (0, 0, 1)$, and its norm is $\varphi^i\varphi_i = r^2 \sin^2\theta$. With the entrainment relations (6) and (7) we can now write the background fluid momenta as

$$\boldsymbol{p}^{\rm n} = m_{\rm b}(\Omega_{\rm n} - \varepsilon_{\rm n}(\Omega_{\rm n} - \Omega_{\rm p}))\boldsymbol{\varphi}, \tag{21}$$

$$\boldsymbol{p}^{\rm p} = m_{\rm b}(\Omega_{\rm p} - \varepsilon_{\rm p}(\Omega_{\rm p} - \Omega_{\rm n}))\boldsymbol{\varphi}. \tag{22}$$

In the following it will be convenient to introduce as a shorthand notation the tilde operator acting on a constituent quantity, Ω_X say, as follows

$$\widetilde{\Omega}_X \equiv \Omega_X - \varepsilon_X(\Omega_X - \Omega_Y), \qquad \text{where} \qquad Y \neq X. \tag{23}$$

This allows us to rewrite the background momenta as

$$\boldsymbol{p}^X = m_{\rm b}\widetilde{\Omega}_X\boldsymbol{\varphi}. \tag{24}$$

We restrict our attention to models with uniform rotation, i.e. $\nabla\Omega_X = 0$. Therefore, the background vorticities are

$$\nabla \times \boldsymbol{p}^X = 2m_{\rm b}\widetilde{\Omega}_X\hat{\boldsymbol{z}} + (\Omega_X - \Omega_Y)\boldsymbol{\varphi} \times \nabla\varepsilon_X, \tag{25}$$

where $\hat{\boldsymbol{z}}$ is the unit vector along the z-axis. We see that, in the general case of a varying entrainment ε_X and different background rotation rates $\Omega_{\rm n} \neq \Omega_{\rm p}$, the vorticities are no longer aligned with the rotation axis. In other words, they acquire a non-zero θ-component and the system is in a state which resembles differential rotation.

As a first step towards a complete understanding of the dynamics of rotating two-fluid systems, we will focus on one of the simplest possibilities. We make the assumption that the entrainment ε_X is constant throughout the star, which means that we have $\nabla\varepsilon_X = 0$ and therefore also $\nabla\widetilde{\Omega}_X = 0$. We note that assuming both entrainment parameters ε_X to be constant also requires a constant proton fraction $x_{\rm p}$. In the following we therefore consider a non-stratified neutron-star model (i.e. $\nabla x_{\rm p} = 0$) with constant entrainment. This model is admittedly simplistic but, as we will see in the following, it nevertheless allows for a rich phenomenology.

4 LINEAR OSCILLATIONS

4.1 Oscillation equations in harmonic basis

Assuming uniform rotation and a constant entrainment model as discussed above, the linear perturbation of the equations of motion (16) can be obtained in the form

$$(\partial_t + \Omega_X \pounds_\varphi)\frac{\delta \boldsymbol{p}^X}{m_{\rm b}} + 2\widetilde{\Omega}_X \boldsymbol{\mathcal{C}}_X + \nabla\psi_X = 0, \tag{26}$$

where the Lie derivative here has the explicit form $\pounds_\varphi \delta p_i = \varphi^j\nabla_j\delta p_i + \delta p_j\nabla_i\varphi^j$, and δ represents an Eulerian perturbation. We have defined the Coriolis term $\boldsymbol{\mathcal{C}}_X$ for each of the two fluids as

$$\boldsymbol{\mathcal{C}}_X \equiv \hat{\boldsymbol{z}} \times \delta\boldsymbol{v}_X, \tag{27}$$

and a scalar potential ψ_X representing the 'effective' pressure perturbation, namely

$$m_{\rm b}\psi_X \equiv \delta\mu^X + m_{\rm b}\delta\phi + \left(\boldsymbol{p}^X - \boldsymbol{v}_X\right) \cdot \delta\boldsymbol{v}_X. \tag{28}$$

The background is assumed to be stationary and axisymmetric, so we can look for eigenmode solutions of the form $\mathrm{e}^{\mathrm{i}(\omega t + m\varphi)}$, and the comoving time derivative in equation (26) can be directly replaced by

$$(\partial_t + \Omega_X \pounds_\varphi) \to \mathrm{i}(\omega + m\Omega_X). \tag{29}$$

The practical advantage of using the Lie derivative $\pounds_\varphi$ here is that the substitution $\pounds_\varphi \to \mathrm{i}m$ holds for any geometric object (e.g. a vector as in equation 26) with a φ dependence of the form $\mathrm{e}^{\mathrm{i}m\varphi}$, while for the simple directional derivative $\boldsymbol{\varphi} \cdot \nabla$ this is only true if it is applied to scalars.

Linear perturbation of the conservation equations (14) and (15) leads to

$$\partial_t\delta n_X + \nabla \cdot (n_X\delta\boldsymbol{v}_X + \delta n_X\boldsymbol{v}_X) = 0. \tag{30}$$

In the present analysis we are only interested in inertial modes, which are characterized by frequencies of the order of the rotation rate Ω. Because this frequency is usually much lower than that of the lowest-order p-mode frequency $\omega_{\rm p}$, we can simplify the problem by using the anelastic approximation (which effectively 'filters out' the p modes). As discussed in more detail in Appendix A, the anelastic approximation consists of replacing the conservation equations by

$$\nabla \cdot (n_X\delta\boldsymbol{v}_X) = 0 + \mathcal{O}\left(\frac{\omega^2}{\omega_{\rm p}^2}\right). \tag{31}$$

The lowest-order p-mode frequency $\omega_{\rm p}$ is of the order of the sound crossing frequency, i.e. $\omega_{\rm p} = \mathcal{O}(c_0/R)$, where c_0 is an averaged sound speed and R is the stellar radius. For low-frequency modes such as the inertial modes we can therefore drop the higher-order corrections in equation (31), which account for the 'elasticity' (i.e. compressibility) of matter. In the following we also restrict ourselves to slowly rotating backgrounds. Because

$$n_X = n_X(r) + \mathcal{O}\left(\frac{\Omega^2}{4\pi G\rho_0}\right), \tag{32}$$

the star remains spherical if we neglect the centrifugal deformation. It is important to note the difference between the slow-rotation approximation, which compares the rotation rate Ω to the Kepler limit $\Omega_{\rm K} = \mathcal{O}(\sqrt{4\pi G\rho_0})$, and the anelastic approximation, which is relevant for mode frequencies that are small compared to $\omega_{\rm p}$. The anelastic approximation (31) together with the slow-rotation approximation (32) is effectively equivalent to the formalism used by Lockitch & Friedman (1999) and others in this context, which

proceeds by ordering all quantities in Ω and keeping only terms up to $\mathcal{O}(\Omega)$. The present approach, however, makes it more obvious that there are really two different small quantities (which both scale with Ω) which can be used for consistent approximations. For example, in the next step one could go up to second order in slow rotation (taking into account the centrifugal deformation of the background) while still working at zeroth order in the anelastic approximation, and thus still filtering out high-frequency modes. In the same manner, one could drop the anelastic approximation while still working with a spherical slow-rotation background.

In order to solve the perturbation equations (26) and (31) for inertial modes, we first transform them into a pseudo-one-dimensional problem by expressing all angular dependences in terms of the spherical harmonics $Y_l^m(\theta,\varphi)$. The spherical harmonics are the eigenvectors of the angular Laplacian, namely

$$\nabla^2 Y_l^m(\theta,\varphi) = -\frac{l(l+1)}{r^2} Y_l^m(\theta,\varphi). \tag{33}$$

Because these functions form a complete orthonormal basis, we can expand a scalar field ψ_X as

$$\psi_X(r,\theta,\varphi) = \psi_X^l(r) Y_l^m(\theta,\varphi), \tag{34}$$

where here and in the following automatic summation over repeated 'angular' indices (l, m, ...) applies. Because of the assumption of an axisymmetric background, the various m-contributions can be decoupled, and therefore we can consider each value of m separately. In order to express a vector field in a similar manner, we use the 'harmonic basis' $\{\boldsymbol{R}_l^m, \boldsymbol{S}_l^m, \boldsymbol{T}_l^m\}$, which is defined in terms of the spherical harmonics as

$$\boldsymbol{R}_l^m \equiv Y_l^m \nabla r, \qquad \boldsymbol{S}_l^m \equiv \nabla Y_l^m, \qquad \boldsymbol{T}_l^m \equiv \boldsymbol{S}_l^m \times \nabla r. \tag{35}$$

We can then expand the velocity perturbations $\delta\boldsymbol{v}_X$ as

$$\delta\boldsymbol{v}_X = \frac{W_X^l(r)}{r}\boldsymbol{R}_l^m + V_X^l(r)\boldsymbol{S}_l^m - \mathrm{i}U_X^l \boldsymbol{T}_l^m. \tag{36}$$

Using the entrainment relations (6) and (7), and assuming a constant entrainment model we obtain

$$\frac{\delta \boldsymbol{p}^X}{m_\mathrm{b}} = \delta\boldsymbol{v}_X - \varepsilon_X(\delta\boldsymbol{v}_X - \delta\boldsymbol{v}_Y) = \delta\widetilde{\boldsymbol{v}}_X, \tag{37}$$

where we have used the definition (23) of the tilde operator. This can conveniently be written in the harmonic basis as

$$\frac{\delta \boldsymbol{p}^X}{m_\mathrm{b}} = \frac{\widetilde{W}_X^l}{r}\boldsymbol{R}_l^m + \widetilde{V}_X^l \boldsymbol{S}_l^m - \mathrm{i}\widetilde{U}_X^l \boldsymbol{T}_l^m. \tag{38}$$

The gradient of a scalar field (34) is readily expressed as

$$\nabla\psi_X = \psi_X^{l\,\prime}(r)\boldsymbol{R}_l^m + \psi_X^l(r)\boldsymbol{S}_l^m, \tag{39}$$

where the prime represents a radial derivative. The expression for the Coriolis terms (27) in the harmonic basis is found after a straightforward, but laborious, calculation to be given by

$$\begin{aligned}\boldsymbol{\mathcal{C}}_X = &-\frac{\mathrm{i}}{r}\left(mV_X^l + \beta_k^l U_X^k\right)\boldsymbol{R}_l^m \\ &-\frac{\mathrm{i}}{l(l+1)}\left(mW_X^l + mV_X^l + \gamma_k^l U_X^k\right)\boldsymbol{S}_l^m \\ &-\frac{1}{l(l+1)}\left(\beta_l^k W_X^k + mU_X^l + \gamma_k^l V_X^k\right)\boldsymbol{T}_l^m,\end{aligned} \tag{40}$$

where we sum over the repeated 'angular' indices (k and l), and the constant matrices β_l^k and γ_k^l are defined as

$$\beta_l^k \equiv l\,Q_{l+1}\delta_{k,l+1} - (l+1)Q_l\delta_{k,l-1}, \tag{41}$$

$$\gamma_k^l \equiv (l^2-1)Q_l\delta_{k,l-1} + l(l+2)Q_{l+1}\delta_{k,l+1}, \tag{42}$$

with the usual definition

$$Q_l \equiv \sqrt{\frac{l^2-m^2}{4l^2-1}}. \tag{43}$$

4.2 The general eigenmode equations

Putting all the pieces together, we can now express the complete system of equations (26) and (31) in the harmonic basis as

$$rW_X^{l\,\prime} + \left(1 + r\frac{n_X'}{n_X}\right)W_X^l - l(l+1)V_X^l = 0, \tag{44}$$

$$\kappa_X\widetilde{W}_X^l - 2\left(mV_X^l + \beta_k^l U_X^k\right) = 2r\widehat{\psi}_X^{l\,\prime}, \tag{45}$$

$$\kappa_X\widetilde{V}_X^l - \frac{2}{l(l+1)}\left(mW_X^l + mV_X^l + \gamma_k^l U_X^k\right) = 2\widehat{\psi}_X^l, \tag{46}$$

$$\kappa_X\widetilde{U}_X^l - \frac{2}{l(l+1)}\left(\beta_l^k W_X^k + mU_X^l + \gamma_k^l V_X^k\right) = 0, \tag{47}$$

where we defined

$$\kappa_X \equiv \frac{\omega + m\Omega_X}{\widetilde{\Omega}_X}, \qquad \text{and} \qquad \widehat{\psi}_X^l \equiv \frac{\mathrm{i}}{2\widetilde{\Omega}_X}\psi_X^l. \tag{48}$$

We note that this definition of the dimensionless frequencies κ_X reduces to the usual single-fluid definition $\kappa = (\omega + m\Omega)/\Omega$ in the case of comoving fluids, or in the absence of entrainment. In both of these cases we have $\widetilde{\Omega}_X \to \Omega_X$ as seen from the definition (23).

The boundary conditions at the centre of the star ($r = 0$) consist of the regularity requirement of the harmonic expansion (34) and (36), which implies the asymptotic conditions

$$W_X^l \sim W_X^l \sim U_X^l \sim \psi_X \sim \mathcal{O}(r^l) \qquad \text{as} \qquad r \to 0. \tag{49}$$

At the surface ($r = R$) we require another regularity condition due to the divergent term n_X'/n_X in the conservation equations (44). As discussed in Appendix A, this is a consequence of the anelastic approximation. The resulting surface boundary condition is therefore

$$W_X(R) = 0, \tag{50}$$

i.e. the radial displacement vanishes at the surface. For models with a vanishing surface density we do not need to impose an explicit condition on the pressure variation at the surface, as for the Lagrangian pressure perturbation δP we have

$$\Delta P = \delta P + \boldsymbol{\xi}\cdot\nabla P = \delta P = \sum n_X \delta\mu^X, \tag{51}$$

where $\boldsymbol{\xi}$ is the displacement vector of the perturbation. The vanishing of δP is therefore ensured provided that $\delta\mu^X$ are regular at the surface. As our numerical scheme can only find such regular solutions, this boundary condition is implicitly guaranteed to hold.

4.3 Special case: zero entrainment

We note that the only coupling between the neutrons ($X = \mathrm{n}$) and the protons ($X = \mathrm{p}$) in the eigenvalue system (44)–(47) is caused by the entrainment, cf. the definition of the tilde operator (23). In the case of zero entrainment, i.e. $\varepsilon_\mathrm{n} = \varepsilon_\mathrm{p} = 0$, we obtain two uncoupled eigenvalue systems. Both systems are formally identical, and therefore both have the same solutions for κ_X, i.e.

$$\kappa_\mathrm{n} = \kappa_\mathrm{p} = \kappa_\mathrm{ord}, \tag{52}$$

where $\kappa_{\rm ord}$ represents the single-fluid solutions. However, from the definition (48) we see that these correspond to different mode frequencies when the rotation rates of the two fluids are different, i.e.

$$\omega_{\rm n} = (\kappa_{\rm ord} - m)\,\Omega_{\rm n}, \qquad \text{and} \qquad \omega_{\rm p} = (\kappa_{\rm ord} - m)\,\Omega_{\rm p}, \tag{53}$$

which implies that these two solutions cannot form a single mode solution when $\Omega_{\rm n} \neq \Omega_{\rm p}$. The two modes in this case therefore correspond to only one of the two fluids oscillating while the other fluid is at rest, i.e.

$$\omega = \omega_{\rm n} : \delta\boldsymbol{v}_n \neq 0, \qquad \text{and} \qquad \delta\boldsymbol{v}_{\rm p} = 0, \tag{54}$$

$$\omega = \omega_{\rm p} : \delta\boldsymbol{v}_n = 0, \qquad \text{and} \qquad \delta\boldsymbol{v}_{\rm p} \neq 0. \tag{55}$$

From the fact that one of the two fluid amplitudes necessarily vanishes when $\varepsilon \to 0$ we deduce that the corresponding amplitude will actually change sign at this point. We can therefore conjecture that if the two fluids were predominantly in phase before crossing $\varepsilon = 0$, then they will be predominantly in counter-phase afterwards and vice versa. We will see in Section 6 that our numerical results agree perfectly with this conjecture.

4.4 The r-mode subclass

The subclass of purely axial inertial modes, commonly referred to as r modes, has generated a lot of interest due to its strong instability with respect to gravitational waves (Andersson 1998; Friedman & Morsink 1998). Therefore, it is interesting to see if this subclass still exists in the superfluid case, and how its properties are modified. A purely axial velocity perturbation is proportional to $\boldsymbol{T}_l^m$, so we set $W_X^l = V_X^l = 0$. In this case, equations (44)–(47) reduce to

$$2\widetilde{\Omega}_X \beta_k^l U_X^k + {\rm i}r\psi_X^{l'} = 0, \tag{56}$$

$$2\widetilde{\Omega}_X \gamma_k^l U_X^k + {\rm i}l(l+1)\psi_X^l = 0, \tag{57}$$

$$\frac{1}{2}\kappa_X l(l+1)\widetilde{U}_X^l - mU_X^l = 0. \tag{58}$$

While the first two equations (56) and (57) allow us to calculate the eigenfunctions U_X^l and ψ_X^l, they do not constrain the eigenvalue in any way. The third equation (58), however, leads to an algebraic constraint for the existence of a non-trivial axial solution. In order to find this constraint, we use the explicit expressions for equation (58) for the two fluids, i.e.

$$\frac{1}{2}l(l+1)\kappa_{\rm n}\left[(1-\varepsilon_{\rm n})U_{\rm n}^l + \varepsilon_{\rm n}U_{\rm p}^l\right] - mU_{\rm n}^l = 0, \tag{59}$$

$$\frac{1}{2}l(l+1)\kappa_{\rm p}\left[(1-\varepsilon_{\rm p})U_{\rm p}^l + \varepsilon_{\rm p}U_{\rm n}^l\right] - mU_{\rm p}^l = 0, \tag{60}$$

from which we can eliminate the U_X^l (assumed non-zero) to obtain the following dispersion relation for superfluid r modes

$$\begin{aligned}&[l(l+1)(1-\varepsilon_{\rm n})(\omega + m\Omega_{\rm n}) - 2m\widetilde{\Omega}_{\rm n}]\\ &\quad\times[l(l+1)(1-\varepsilon_{\rm p})(\omega + m\Omega_{\rm p}) - 2m\widetilde{\Omega}_{\rm p}]\\ &\quad - l^2(l+1)^2\varepsilon_{\rm n}\varepsilon_{\rm p}(\omega + m\Omega_{\rm n})(\omega + m\Omega_{\rm p}) = 0.\end{aligned} \tag{61}$$

We note that this corrects the dispersion relation that was used by Andersson, Comer & Prix (2003) in a discussion of the superfluid two-stream instability of the r modes.

5 THE COROTATING CASE $\Omega_{\rm n} = \Omega_{\rm p}$

Before turning to the numerical solution of the general case with $\Omega_{\rm n} \neq \Omega_{\rm p}$, it is instructive to study the special case of two corotating fluids, where we have $\widetilde{\Omega}_X = \Omega$. The linearized perturbation equations (26) and (31) then take the form

$${\rm i}\kappa[\delta\boldsymbol{v}_X - \varepsilon_X(\delta\boldsymbol{v}_X - \delta\boldsymbol{v}_Y)] + 2\boldsymbol{\mathcal{C}}_X + \frac{\nabla\psi_X}{\Omega} = 0, \tag{62}$$

$$\nabla\cdot(n_X\delta\boldsymbol{v}_X) = 0, \tag{63}$$

where we have defined

$$\kappa \equiv \frac{\omega + m\Omega}{\Omega}, \tag{64}$$

which is the usual dimensionless frequency of inertial modes in the corotating frame. It is interesting to see under which conditions this system can be separated into purely comoving and counter-moving modes. We therefore introduce the usual variables corresponding to these two mode-classes, namely

$$\begin{aligned}\delta\boldsymbol{\Delta} &\equiv \delta\boldsymbol{v}_{\rm p} - \delta\boldsymbol{v}_{\rm n}, & \delta\beta &\equiv \psi_{\rm p} - \psi_{\rm n},\\ \delta\boldsymbol{v} &\equiv x_{\rm p}\delta\boldsymbol{v}_{\rm p} + x_{\rm n}\delta\boldsymbol{v}_{\rm n}, & \delta\mu &\equiv x_{\rm p}\psi_{\rm p} + x_{\rm n}\psi_{\rm n}.\end{aligned} \tag{65}$$

In terms of these variables the oscillation equations can be rewritten as

$$\nabla\cdot(n\delta\boldsymbol{v}) = 0, \tag{66}$$

$${\rm i}\kappa\delta\boldsymbol{v} + 2\hat{\boldsymbol{z}}\times\delta\boldsymbol{v} + \nabla\delta\mu = \delta\beta\nabla x_{\rm p}, \tag{67}$$

$$\nabla\cdot(nx_{\rm n}x_{\rm p}\delta\boldsymbol{\Delta}) = -n\delta\boldsymbol{v}\cdot\nabla x_{\rm p}, \tag{68}$$

$${\rm i}\gamma^{-1}\kappa\delta\boldsymbol{\Delta} + 2\hat{\boldsymbol{z}}\times\delta\boldsymbol{\Delta} + \nabla\delta\beta = 0, \tag{69}$$

where we have defined

$$\gamma \equiv \frac{1}{1-\varepsilon_{\rm n}-\varepsilon_{\rm p}} = \left(1 - \frac{\varepsilon}{1-x_{\rm p}}\right)^{-1}. \tag{70}$$

We see that the variables $\{\delta\boldsymbol{v},\ \delta\mu\}$, which are characteristic of 'ordinary'-type modes, decouple from the 'superfluid' variables $\{\delta\boldsymbol{\Delta},\ \delta\beta\}$, if and only if the background model is not stratified, i.e. if $\nabla x_{\rm p} = 0$. This is exactly the same condition that was found in the case of a static superfluid neutron star (Prix & Rieutord 2002). We further see that in the non-stratified case the equations governing the two mode-families are equivalent, and the 'ordinary'-type mode frequencies $\kappa_{\rm ord}$ are therefore related to the 'superfluid'-type ones by

$$\kappa_{\rm sf} = \gamma\kappa_{\rm ord}. \tag{71}$$

It is well known (Bryan 1889) that the inertial mode frequencies $\kappa\Omega$ of an incompressible fluid are bounded (and form a dense set) in the interval $[-2\Omega, 2\Omega]$. In the compressible case, we still expect this to hold approximately. This will therefore also be true for the 'ordinary'-type modes in the corotating case, but relation (71) shows that the corresponding interval for the 'superfluid'-type modes will be governed by the factor γ. This scalefactor depends only on the proton fraction $x_{\rm p}$ and the entrainment ε, and can, in principle, take any value between $[-\infty, +\infty]$. For $\varepsilon < 0$ we have $\gamma \in (0, 1)$, i.e. the 'superfluid'-type mode frequencies lie closer to the origin than their 'ordinary'-type counterpart, and they are bounded by a smaller interval than the 'ordinary' modes. For $\varepsilon > 0$ on the other hand, the 'superfluid'-type mode frequencies lie further away from the origin than their 'ordinary' counterparts and their bounding interval is

larger. We also note that the 'ordinary'-type modes are independent of the entrainment (in these non-stratified models), as expected from their strictly comoving character. If we express the scalefactor (70) in terms of the alternative entrainment parameter ϵ as defined in equation (13), we find

$$\gamma = 1 + \frac{\epsilon}{x_{\rm p}}. \tag{72}$$

Therefore, we see that the 'superfluid'-type mode frequencies are linear in ϵ. This has been found previously for the r-mode subclass by Andersson & Comer (2001). It was also observed numerically for inertial modes by Lee & Yoshida (2003) and Yoshida & Lee (2003a), although only as an 'almost' linear dependence. This slight discrepancy is not surprising as their background model is stratified (i.e. $x_{\rm p}$ is not constant) and the above decoupling of the mode families is therefore expected to hold only approximately.

5.1 The r modes of the corotating model

In the case of a corotating background, the r-mode dispersion relation (61) reduces to

$$[(1-\varepsilon_{\rm n})\kappa - \kappa_{\rm ord}][(1-\varepsilon_{\rm p})\kappa - \kappa_{\rm ord}] - \varepsilon_{\rm n}\varepsilon_{\rm p}\kappa^2 = 0, \tag{73}$$

where

$$\kappa_{\rm ord} \equiv \frac{2m}{l(l+1)} \tag{74}$$

is the standard single-fluid r-mode frequency. Solving the quadratic dispersion relation we find that the two r-mode frequencies of the superfluid problem are

$$\kappa = \{\kappa_{\rm ord}, \gamma\kappa_{\rm ord}\}, \tag{75}$$

in agreement with the general relation (71).

In order to find the corresponding eigenfunctions, we eliminate ψ^l_X from equations (56) and (57) to obtain

$$\frac{l-1}{l} Q^m_l \left[U_X^{l-1\prime} - l\frac{U_X^{l-1}}{r} \right] + \frac{l+2}{l+1} Q^m_{l+1} \left[U_X^{l+1\prime} + (l+1)\frac{U_X^{l+1}}{r} \right] = 0. \tag{76}$$

This equation has to hold for every $l \geqslant m$, and we can therefore extract the two simultaneous conditions

$$Q^m_{l+1} \left[U_X^{l\prime} - (l+1)\frac{U_X^l}{r} \right] = 0, \tag{77}$$

$$Q^m_l \left[U_X^{l\prime} + l\frac{U_X^l}{r} \right] = 0, \tag{78}$$

for which the only non-trivial and non-singular solution is

$$U^l_X = C_X r^{l+1}, \qquad \text{with} \qquad m = l. \tag{79}$$

Substituting this eigenfunction and the eigenvalues (75) back into (58), we find the following relation between the two amplitudes

$$\kappa = \kappa_{\rm ord} : C_{\rm p} = C_{\rm n}, \tag{80}$$

$$\kappa = \gamma\kappa_{\rm ord} : C_{\rm p} = -\frac{n_{\rm n}}{n_{\rm p}} C_{\rm n}, \tag{81}$$

which corresponds to purely comoving and counter-moving r modes, respectively.

6 NUMERICAL RESULTS FOR THE GENERAL CASE $\Omega_{\rm n} \neq \Omega_{\rm p}$

In the following we choose the proton rotation rate $\Omega_{\rm p}$ as the 'reference' rotation rate. This choice is motivated by the fact that the observed rotation of neutron stars (via pulsar emission) is thought to be related to the charged components (assumed to corotate with the crust), while the rotation rate $\Omega_{\rm n}$ of the superfluid neutrons is not directly observable. We define the relative rotation rate $\mathcal{R}$ as

$$\mathcal{R} \equiv \frac{\Omega_{\rm n} - \Omega_{\rm p}}{\Omega_{\rm p}}. \tag{82}$$

With these definitions we can write equation (23) as

$$\widetilde{\Omega}_{\rm n} = \Omega_{\rm p}[1 + (1-\varepsilon_{\rm n})\mathcal{R}], \tag{83}$$

$$\widetilde{\Omega}_{\rm p} = \Omega_{\rm p}[1 + \varepsilon_{\rm p}\mathcal{R}]. \tag{84}$$

Further introducing

$$2\nu_{\rm n} \equiv \frac{1}{1+(1-\varepsilon_{\rm n})\mathcal{R}}, \qquad \text{and} \qquad 2\nu_{\rm p} \equiv \frac{1}{1+\varepsilon_{\rm p}\mathcal{R}}, \tag{85}$$

we can express κ_X defined in equation (48) as

$$\kappa_{\rm n} = 2\nu_{\rm n}\kappa_0 + 2m\nu_{\rm n}\mathcal{R}, \tag{86}$$

$$\kappa_{\rm p} = 2\nu_{\rm p}\kappa_0, \tag{87}$$

where κ_0 is a dimensionless 'reference frequency' of the mode, which we define as

$$\kappa_0 \equiv \frac{\omega + m\Omega_{\rm p}}{\Omega_{\rm p}}, \tag{88}$$

in analogy with the usual single-fluid definition. With these definitions we can write the system of equations (44)–(47) as a one-dimensional infinite eigenvalue problem for κ_0 in the form

$$\sum_{l=|m|}^{\infty} \widehat{A}_l \Psi^l = \kappa_0 \sum_{l=|m|}^{\infty} \widehat{B}_l \Psi^l, \tag{89}$$

where $\widehat{A}_l$ and $\widehat{B}_l$ are linear operators and Ψ^l is the eigenvector

$$\Psi^l = \left\{ W^l_{\rm n}, W^l_{\rm p}, V^l_{\rm n}, V^l_{\rm p}, U^l_{\rm n}, U^l_{\rm p}, \widehat{\psi}^l_{\rm n}, \widehat{\psi}^l_{\rm p} \right\}. \tag{90}$$

The explicit form of these equations is given in Appendix B. By taking the sum over l only up to a finite value $l_{\rm max}$, we can solve the resulting finite eigenvalue problem using the LSB spectral solver, which is based on the efficient incomplete Arnoldi–Chebychev algorithm. This is the same method that Prix & Rieutord (2002) used to study non-radial oscillations of non-rotating superfluid neutron stars.

Most of the numerical calculations in the following have been performed for both a uniform-density background (i.e. polytropic index $N = 0$) and a polytropic background with $N = 1$ (for each of the fluids). The results are quite similar and we therefore only present the polytropic case here. Furthermore, we only considered the case $m = 2$, which is expected to be the most relevant for gravitational-wave emission. The results for higher values of m are not expected to show any qualitative differences. In all of the following sections except for Section 6.4, we use a neutron-star model with 'canonical' values $x_{\rm p} = 0.1$ for the proton fraction and $\varepsilon = 0.6$ for the entrainment, which conveniently results in a scaling factor (70) of $\gamma = 3$. This choice of parameters is referred to as 'model I'. In Section 6.4 on the two-stream instability, on the other hand, we will choose these values to be $x_{\rm p} = 0.2$ and $\varepsilon = -2$, which leads to $\gamma \approx 0.2857$, and we call this 'model II'. The parameters of these two neutron-star models are

Table 1. Parameters of the two neutron-star models studied here.

Model	x_p	ε	γ
I	0.1	0.6	3.0
II	0.2	−2.0	0.2857

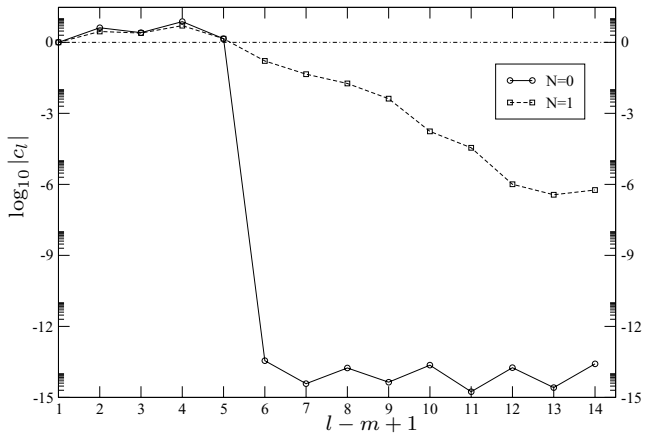

Figure 1. Angular convergence of the ('ordinary') inertial mode with $m=2$ and $j\equiv l_0-m+1=5$ (which we label ${}^{5}_{2}I^{\rm ord}_{(1)}$) at $\mathcal{R}=0$ for the homogeneous background model ($N=0$) and the $N=1$ polytrope. The plotted quantity c_l represents the magnitude of the harmonic expansion coefficients (34) and (36) of the eigenmode.

summarized in Table 1. For the low-order inertial modes considered in this paper a radial resolution of 30 Chebychev polynomials and an angular resolution of about 10 spherical harmonics is used in most cases, which proves sufficient to obtain a numerical precision of the order of 10^{-6}. In the case of r modes, we compared our numerical results to a direct evaluation of the dispersion relation (61) and found an agreement better than 10^{-6} in all cases considered. In the corotating case ($\mathcal{R}=0$) our numerical results for the 'ordinary' modes agree up to the given precision $\sim 10^{-6}$) with the single-fluid results in the literature (e.g. Lockitch & Friedman 1999), and the 'superfluid' modes satisfy the analytical relation (71) as expected.

6.1 Angular convergence and inertial-mode labelling

It was shown by Lockitch & Friedman (1999) that for $m\neq 0$ the lowest non-zero l-coefficient in the harmonic expansions (34) and (36) is necessarily $l=|m|$. Furthermore, in the case of a uniform density background model (i.e. $N=0$), it is known that the harmonic expansion (36) of the solution $\delta\boldsymbol{v}$ stops at a finite l_0. In fact, the corresponding coefficients can be calculated analytically. There are always exactly $j\equiv l_0-|m|+1$ mode-solutions for any given $m\neq 0$ and $l_0\geqslant|m|$. In the case of a polytropic background with $N=1$ the solution turns out to be quite similar to the uniform case, except that the expansion does not stop after a finite number of terms. Instead it converges exponentially beyond $l=l_0$. This behaviour is illustrated in Fig. 1, which shows the angular expansion coefficients of the (axial-led, $m=2$) inertial mode with $\kappa_0=-1.308$ for $N=0$ and the analogous mode $\kappa_0=-1.43392$ for $N=1$. We see that in the uniform background case there is a sharp drop after $j=5$, as the higher-order coefficients are analytically zero, while in the polytropic case we observe an exponential falloff. The quantitative and qualitative similarity to the uniform model allows us to associate

Table 2. Inertial-mode frequencies κ_0 of the polytropic model I (cf. Table 1) for backgrounds with relative rotation $\mathcal{R}=0$ and for $\mathcal{R}=0.1$, respectively.

${}^{j}_{m=2}I_{(n)}$	$\kappa_0^{\rm ord}\vert_{\mathcal{R}=0}$	$\kappa_0^{\rm sf}\vert_{\mathcal{R}=0}$	$\kappa_0^{\rm ord}\vert_{\mathcal{R}=0.1}$	$\kappa_0^{\rm sf}\vert_{\mathcal{R}=0.1}$
${}^{1}I_{(1)}$	0.666 667	2.000 000	0.545 300	2.108 033
${}^{2}I_{(1)}$	−0.556 592	−1.669 775	−0.781 724	−1.800 487
${}^{2}I_{(2)}$	1.100 026	3.300 077	1.018 492	3.489 617
${}^{3}I_{(1)}$	−1.025 883	−3.077 648	−1.295 019	−3.295 758
${}^{3}I_{(2)}$	0.517 337	1.552 012	0.381 944	1.632 260
${}^{3}I_{(3)}$	1.357 781	4.073 343	1.299 684	4.311 618

the modes of the polytropic model with corresponding modes of the uniform model. In case of doubt it should always be possible to associate modes via a continuous transformation of N. We can therefore conveniently label the modes by their 'quantum numbers' m, j and an additional index $n\in[1,j]$ accounting for the j different solutions at given m and j. As a convention we choose to order the modes by increasing frequency κ_0, so we label the inertial modes as

$$ {}^{j}_{m}I_{(n)} : {}^{j}_{m}I_{(1)} < {}^{j}_{m}I_{(2)} < \cdots < {}^{j}_{m}I_{(j)}, \tag{91}$$

where the inequalities obviously refer to the eigenfrequency κ_0 of the corresponding mode. For the sake of reference we show the frequencies κ_0 of the six lowest-order inertial modes in Table 2, both for a corotating background $\mathcal{R}=0$ and for $\mathcal{R}=0.1$. We note that the values for $\kappa_0^{\rm ord}|_{\mathcal{R}=0}$ agree up to the given precision with previous results in the literature, (e.g. Lockitch & Friedman 1999). We also note that the 'superfluid' frequencies in the corotating case satisfy the scaling relation (71) at $\mathcal{R}=0$ with $\gamma=3.0$ (cf. Table 1), while this relation naturally does not hold for $\mathcal{R}\neq 0$.

6.2 The effect of relative rotation $\mathcal{R}$

We have seen in Section 5 that in the corotating case the inertial modes of non-stratified stars can be separated into purely comoving and counter-moving families. This is no longer true when we allow for a non-zero relative rotation $\mathcal{R}\neq 0$. Similar to stratification (cf. Prix & Rieutord 2002), the relative rotation introduces a coupling between these mode families, leading to a deviation from the strictly comoving and counter-moving nature of the modes. This is shown in Fig. 2.

Compared to the effect of stratification, however, the mode coupling induced by the relative rotation $\mathcal{R}$ (in the absence of

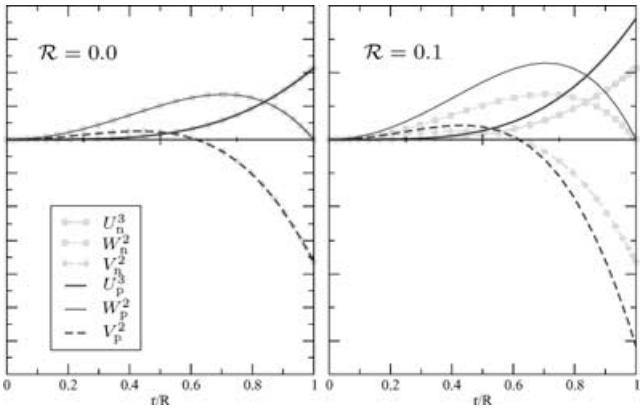

Figure 2. The polar-led 'ordinary' inertial mode ${}^{2}_{2}I^{\rm ord}_{(1)}$ for model I with a corotating background $\mathcal{R}=0$ (left panel) and $\mathcal{R}=0.1$ (right panel). The next higher l-contributions are one order of magnitude smaller and are not included in this graph.

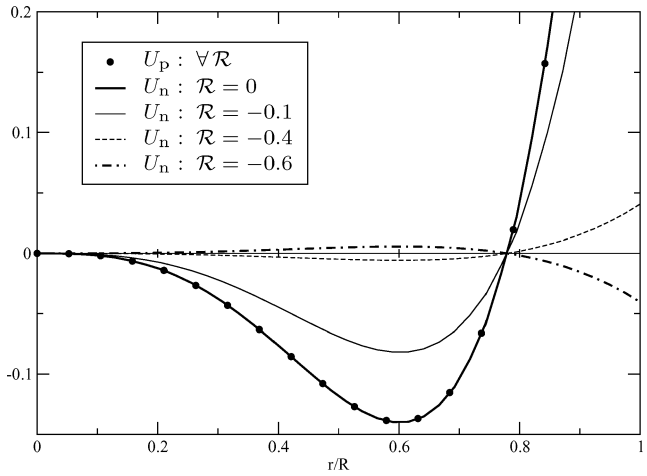

Figure 3. Neutron and proton amplitudes for different relative rotations $\mathcal{R}$. The plot shows the $l = 2$ components U_n and U_p of the mode ${}^3_2I^{ord}_{(2)}$ for $\mathcal{R} = 0$, -0.1, -0.4 and -0.6. The normalization is such that $U_p(R) = 1$, for which U_p is seen to be invariant under changes of $\mathcal{R}$.

stratification) seems to be of a much weaker nature. Although the two fluids are no longer strictly comoving or counter-moving, they always have a well-defined phase relation, in the sense that they are either strictly in phase or in counter-phase. Changing $\mathcal{R}$ does not change the position of the nodes of the mode. This can be seen in Fig. 3 which illustrates the transition of the ${}^3_2I^{ord}_{(2)}$ mode being in phase to being in counter-phase when varying $\mathcal{R}$. Furthermore, this coupling does not lead to general avoided crossings between inertial modes, as can be seen in Fig. 4 in which we show the mode frequencies of the lowest-order inertial modes as functions of the relative rotation rate $\mathcal{R}$. A striking feature of this graph is that there are two common crossing points for the mode frequencies. This can be understood as follows. The system of equations (B1)–(B8) has a singularity when $\nu_X \to \infty$ for $X = n$ or $X = p$. We see from equation (85) that this happens at the relative rotation rates

$$\mathcal{R} = -\frac{1}{1-\varepsilon_n} \qquad \text{and} \qquad \mathcal{R} = -\frac{1}{\varepsilon_p},$$

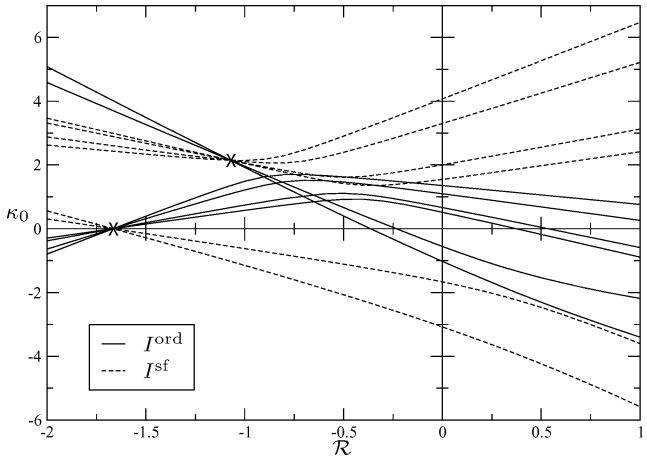

Figure 4. Frequencies κ_0 of 'ordinary' I^{ord} and 'superfluid' I^{sf} inertial modes with $m = 2$ as functions of the relative rotation rate $\mathcal{R}$ for the polytropic ($N = 1$) background model I. The two common crossing points (94) are marked by 'x'. The modes presented here are the six lowest-order inertial modes, ${}^1_2I_{(1)}$ to ${}^3_2I_{(3)}$.

respectively. At these singular points the system of equations reduces to the following constraints:

$$\nu_n \to \infty : \kappa_0 = -m\mathcal{R}, \qquad \text{or} \qquad W^l_n = -\frac{\varepsilon_n}{1-\varepsilon_n} W^l_p, \tag{92}$$

$$\nu_p \to \infty : \kappa_0 = 0, \qquad \text{or} \qquad W^l_p = -\frac{\varepsilon_p}{1-\varepsilon_p} W^l_n, \tag{93}$$

and similar amplitude constraints hold for V^l_X and U^l_X. The two common crossing points therefore have to be

$$(\mathcal{R}, \kappa_0) = \left\{ \left(-\frac{1}{\varepsilon_p}, 0 \right), \left(\frac{1}{1-\varepsilon_n}, -m\mathcal{R} \right) \right\}. \tag{94}$$

These points are marked by 'x' in our various frequency plots. The solutions at these critical relative rotation rates fall into two classes: modes that cross at the common crossing point, and modes that satisfy the amplitude relations (92) or (93). These analytical results agree perfectly well with the numerical findings and provide a good consistency check of our numerical results. We note that while in Fig. 4 it seems as if each of the modes necessarily passes through one of the two crossing points, this is not generally the case, as will be seen in Fig. 7 for a different choice of parameters.

It is interesting to note that the two critical relative rotation rates correspond to the vanishing of the angular momentum of one of the two fluids, i.e. $\nu_n \to \infty$ corresponds to $\boldsymbol{p}^n = 0$ and $\nu_p \to \infty$ is equivalent to $\boldsymbol{p}^p = 0$. This is obviously an effect of the entrainment – the fluid is rotating but has zero angular momentum. As a result, the Coriolis force acting on this fluid vanishes and the mode becomes stationary in the reference frame of the respective fluid. As we have chosen Ω_p as our reference rotation, we find $\kappa_0 = 0$ for $\boldsymbol{p}^p = 0$. The non-zero crossing frequency $\kappa_0 = -m\mathcal{R}$ for $\boldsymbol{p}^n = 0$ simply corresponds to zero frequency in the neutron-frame observed in the proton-frame.

While there are no general avoided crossings, the coupling induced by $\mathcal{R}$ does lead to avoided crossings between corresponding 'mode pairs', i.e. between the 'ordinary' mode and its 'superfluid' counterpart, as can be seen in Fig. 5. We note that the labelling I^{ord} and I^{sf} used in Fig. 4 to refer to 'ordinary' or 'superfluid' modes is defined by continuing the mode from $\mathcal{R} = 0$. This labelling can be misleading, however, as for $\mathcal{R} \neq 0$ it does not reflect the comoving or counter-moving nature of the mode. Neither does it imply the mode to be in phase or in counter-phase, as can be seen from Fig. 3. In Fig. 5 and in the following it will often be more interesting to indicate the phase character of a mode, so we will write I_+ for modes with in-phase fluid motion, and I_- for modes where the fluids are in counter-phase. As we have already seen in Fig. 3, the relative phase is not an invariant property of the 'ordinary' or 'superfluid' mode families. For example, in Fig. 5 the 'superfluid' modes are always in counter-phase, while the 'ordinary' mode is in phase in a certain region but in counter-phase in another. We note, however, that the ordinary mode necessarily has to be in phase in $\mathcal{R} = 0$, as we know analytically (see Section 5) that at this point the two mode-families have strict comoving and counter-moving character.

Let us consider the relation between the pattern speed $\dot{\varphi} = -\omega/m$ of the mode and the two rotation rates Ω_n and Ω_p. In particular, we are interested in the region where the pattern speed of the mode lies in between the rotation rates of the two fluids, such that it would appear prograde when viewed in one fluid frame and retrograde in the other. We can see that this 'mixed' region is characterized by the condition

$$\kappa_0(\kappa_0 + m\mathcal{R}) < 0. \tag{95}$$

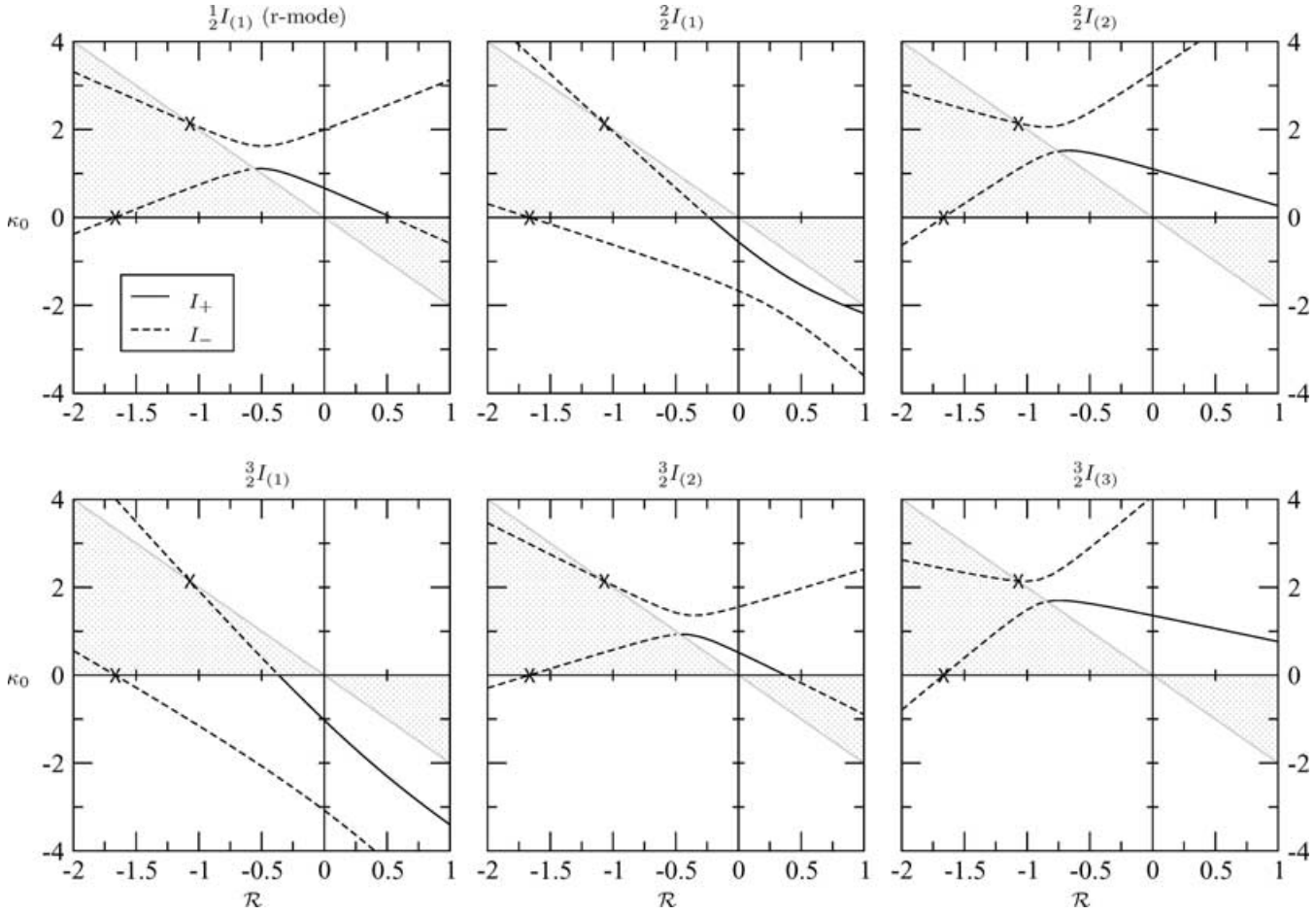

Figure 5. Avoided crossings between 'ordinary' and 'superfluid' (defined at $\mathcal{R} = 0$) inertial modes as functions of the relative rotation rate $\mathcal{R}$. The common crossing points (94) are marked by 'x' and the shaded areas corresponds to the 'mixed' region as defined in equation (95). The labels I_+ and I_- indicate if the two fluids are in phase or in counter-phase, respectively.

This 'mixed' region is indicated in Figs 5 and 7 as a shaded area, and we observe that the change of the phase character of modes only occurs when the mode frequency crosses into or out of the 'mixed' region. There seems to be no phase change, however, if the crossing takes place via one of the two common crossing points (94), which are indicated by 'x' in these figures. We can try to understand this as follows. When a mode crosses into or out of the 'mixed' region, it means that its frequency vanishes and changes sign in one of the two fluid frames. In general, the Coriolis force of the corresponding fluid is non-zero in this point, therefore the frequency can only be zero if the fluid ceases to move. The corresponding fluid eigenfunctions therefore undergo a sign change, which results in the phase change of the mode. In the special case where the crossing occurs via one of the two common crossing points, however, the Coriolis force does vanish at this point and subsequently changes sign, therefore the mode amplitude cannot change sign and the crossing takes place without a phase change.

6.3 Varying the entrainment

In Fig. 6 we have plotted the mode frequencies of background model I as functions of the entrainment ε for a configuration with relative rotation $\mathcal{R} = 0.1$. Similar to the avoided crossings as functions of $\mathcal{R}$ shown in Fig. 5, we observe that there are only 'pairwise' avoided crossings, i.e. between an 'ordinary' and the corresponding 'superfluid' mode. We further note that the crossing of the zero-entrainment axis ($\varepsilon = 0$) is rather special, as can be understood from the discussion in Section 4.3. At $\varepsilon = 0$, one of the two fluid amplitudes is necessarily zero, and therefore the crossing of the $\varepsilon = 0$ axis induces a phase change between the two fluids. This is exactly the behaviour observed numerically for the modes shown in Fig. 6.

We also note that in the corotating case $\mathcal{R} = 0$ we would only find degenerate crossings at $\varepsilon = 0$, because we know analytically that in this case $\gamma = 1$, so that with equation (71) we have $\kappa_{\rm ord} = \kappa_{\rm sf}$. This is a particularity of the non-stratified model, as indicated by similar results for the oscillation modes of static backgrounds models (Prix & Rieutord 2002). Avoided crossings as functions of ε were first suggested by Andersson & Comer (2001) and then first calculated in the relativistic study of (stratified) static models by Andersson, Comer & Langlois (2002). Furthermore, Lee & Yoshida (2003) and Yoshida & Lee (2003a) have observed avoided crossings between inertial modes of corotating (stratified) superfluid models. This is consistent with our results.

6.4 The two-stream instability

It was recently discovered (Andersson, Comer & Prix, in preparation) that superfluid systems may, quite generally, suffer a so-called 'two-stream instability'. In the present context, this instability

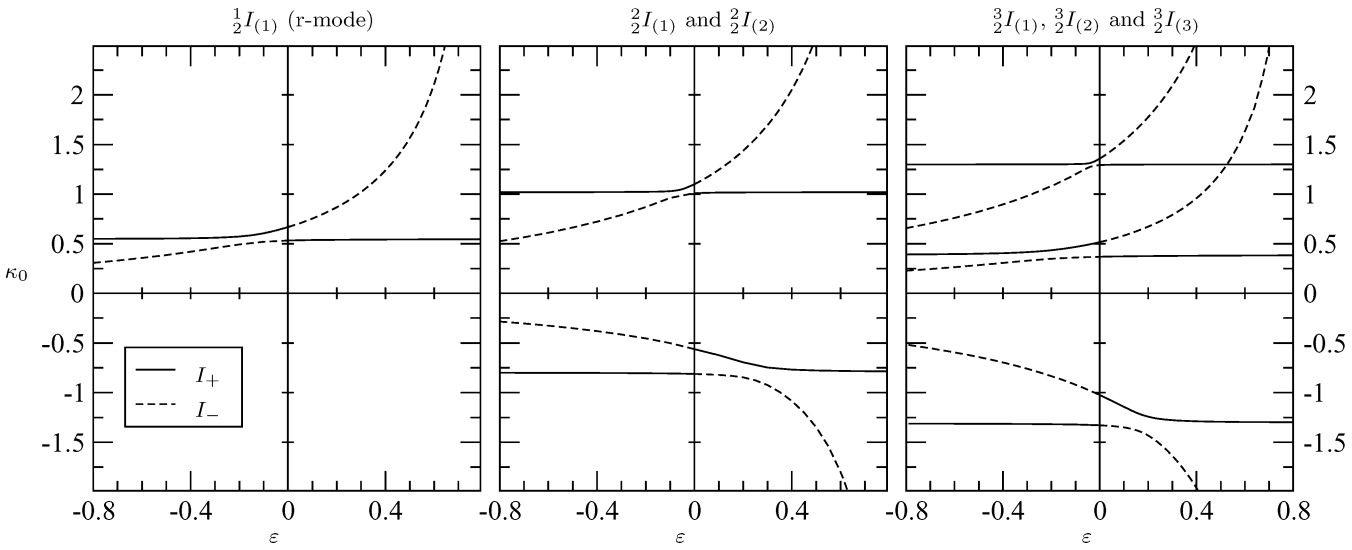

Figure 6. Avoided crossings between 'ordinary' and 'superfluid' $m = 2$ inertial modes as functions of entrainment ε for the background model I and a relative rotation rate of $\mathcal{R} = 0.1$. The labels I_+ and I_- refer to the phase character of the modes.

would set in when the relative velocity between the two fluids exceeds a certain critical level. This mechanism was suggested as a possible mechanism for triggering pulsar glitches (Andersson et al. 2003). Unfortunately, the dispersion relation for superfluid r modes on which the analysis of Andersson et al. (2003) was based is incorrect, affecting the various estimates for the onset and growth of the instability (for a detailed discussion, see Andersson et al., in preparation).

As the general instability mechanism remains sound, we expect to find inertial modes that become unstable beyond a critical relative rotation rate $\mathcal{R}$. For the parameter values chosen for Fig. 5, no such instabilities were observed within the interval $-2 \leqslant \mathcal{R} \leqslant 1$ that was considered. However, using the dispersion relation (61), we can identify a more instability-prone region to be, for example, a proton fraction of $x_\mathrm{p} = 0.2$ and an entrainment of $\varepsilon = -2$, which is our model II (cf. Table 1). In the neutron-star core, the entrainment ε is generally expected to be positive, but a negative entrainment is nevertheless not unphysical. Superfluid ^{4}He, for example, has negative entrainment, and this is also expected to be the case for the neutron superfluid in the neutron-star crust (Carter, Chamel & Haensel, in preparation). While the present example serves only as a consistency check and proof of principle, we emphasize that these parameter values are not completely unphysical. In Fig. 7 we plot the frequencies of the lowest-order inertial modes as functions of the $\mathcal{R}$ for this choice of parameters. We see that now the r mode $^1_1I_{(1)}$, and the inertial modes $^2_2I_{(2)}$ and $^3_2I_{(3)}$ do indeed undergo an instability via the merger of the 'ordinary'-type mode with its 'superfluid' counterpart. After this merger, the two mode-frequencies are complex conjugates, which is to be expected from the time symmetry of the problem. The real part of κ_0 is strictly linear in $\mathcal{R}$ in the instability region. For the present set of parameters, the two common crossing points given by equation (94) are $(\mathcal{R}, \kappa_0) = (0.5, 0)$ and $(-0.6667, 1.3333)$. These points are marked by 'x' in Fig. 7. Interestingly, the instability point of the r mode coincides (up to numerical precision $\sim 10^{-6}$) with one of the common crossing points discussed earlier, namely the one at which the proton-fluid angular momentum vanishes. Using the analytic r-mode dispersion relation (61), we can verify that the instability occurs exactly at the crossing point $(0.5, 0)$. However, this is clearly seen not to be the case for the higher-order inertial modes. We might expect the instabilities to occur in one of the 'mixed' regions, as the mode is then prograde in one fluid frame and retrograde in the other (see, for example, Pierce 1974). This, however, is not always the case, as illustrated in Fig. 8. We see that onset of the instabilities of the $^2_2I_{(2)}$ and $^3_2I_{(3)}$ modes occurs slightly outside the 'mixed' region. Given the numerical precision of $\leqslant 10^{-6}$, this should not be due to numerical errors. This observation serves as a strong motivation for a study into the stability properties of rotating multi-fluid systems. It would be desirable to attempt a derivation of useful instability criteria, e.g. analogous to those derived by Friedman & Schutz (1978) for the single-fluid problem.

7 DISCUSSION

In this paper we have derived the equations that govern inertial modes of a slowly-rotating superfluid neutron-star model using the anelastic and slow-rotation approximations. These equations are more general than those used in previous studies because they allow for general non-corotating backgrounds $\Omega_\mathrm{n} \neq \Omega_\mathrm{p}$. We have discussed analytically the special cases of corotation and zero entrainment. The obtained analytical results were then confirmed by, and thus served as important benchmark tests for, our numerical calculations. We studied numerically the dependence of the mode frequencies on the relative rotation rate and entrainment, and found avoided crossings between mode pairs. The 'phase character' of the modes was found to be rather complex, in the sense that it can change when crossing into or out of a 'mixed region'. In a 'mixed region' the mode frequencies lie in between the two background rotation rates. We have also confirmed, for the first time in a complete mode calculation, the existence of the superfluid two-stream instability. We have studied the onset of this instability as a function of relative rotation rate, and found that, contrary to intuitive expectations, the onset can sometimes take place slightly outside the 'mixed region'.

The complicated problem of oscillations of rotating multi-fluid systems provides many challenges that should inspire future work. More detailed models should allow for stratified backgrounds as this would be closer to a realistic neutron-star model. Stratification is expected to lead to a substantially more complex character of the mode

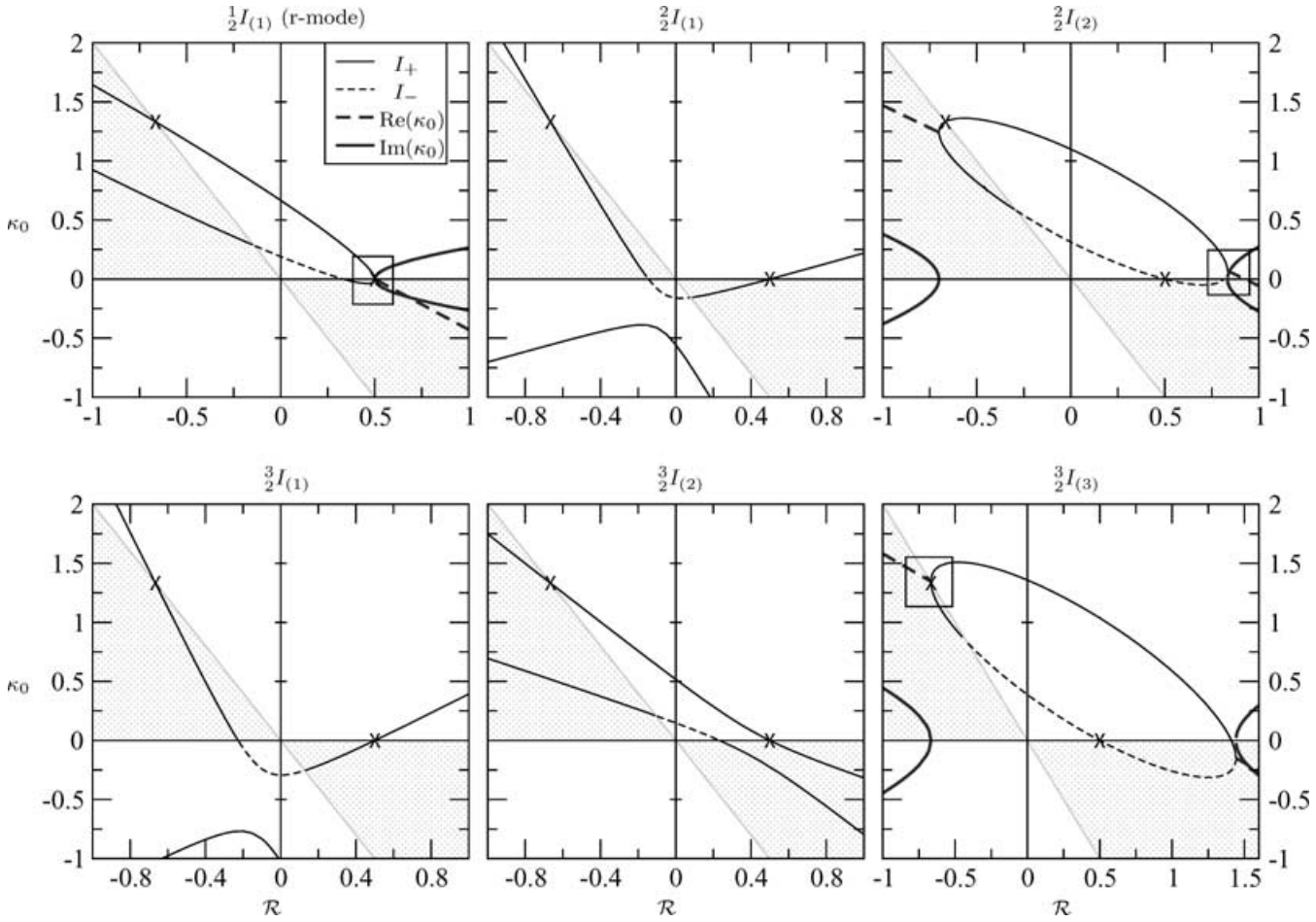

Figure 7. Inertial-mode frequencies as functions of the relative rotation $\mathcal{R}$ for model II (cf. Table 1). The common crossing points (94) are marked by 'x'. Merger of two real frequencies leads to a complex-conjugate pair, and signals the onset of instability. The shaded areas indicate the 'mixed' region as defined in equation (96). The labels I_+ and I_- indicate if the two fluids are in phase or in counter-phase, respectively. The boxes indicate regions that we zoom into in Fig. 8.

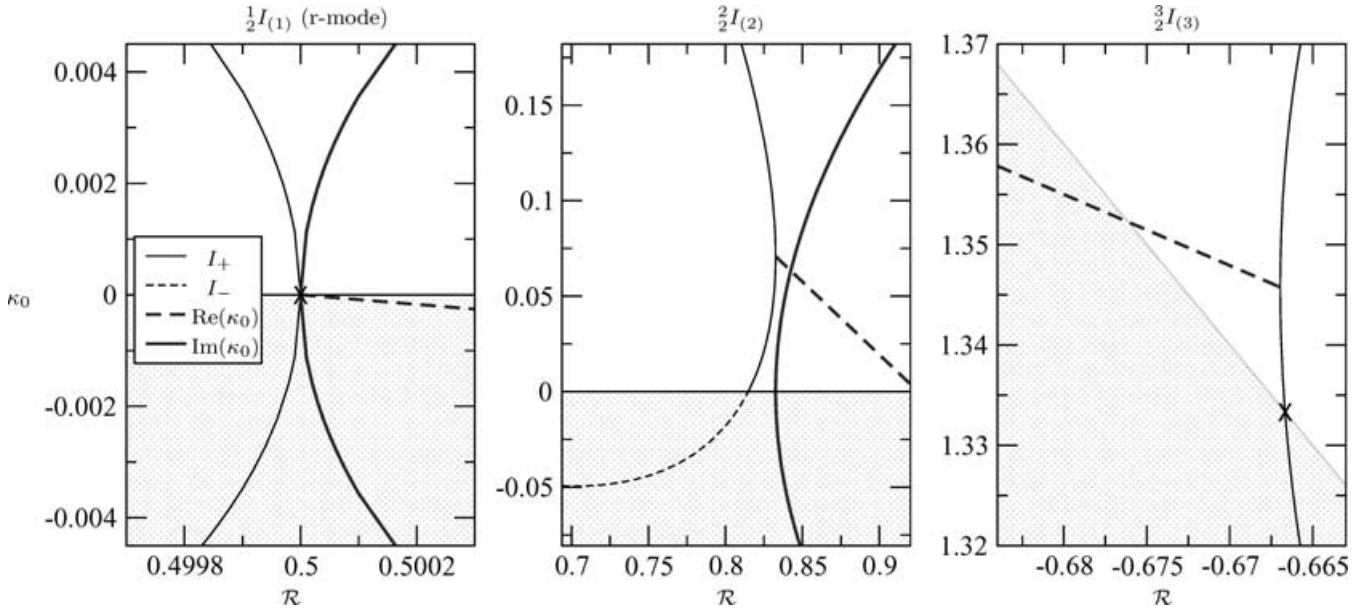

Figure 8. Close-up of the vicinity of the three instability points marked by boxes in Fig. 7. The common crossing points (94) are marked by 'x'. The labels I_+ and I_- indicate if the two fluids are in phase or in counter-phase, respectively.

spectrum. In particular, there is likely to be avoided crossings between all modes and the modes will no longer be of purely 'in-phase' or 'counter-phase' character. This has already been observed in the studies by Lee & Yoshida (2003) and Yoshida & Lee (2003a) in the purely corotating case. It would also be interesting to move beyond both the anelastic approximation and the slow-rotation approximation, in order to be able to consider rapidly spinning stars. We should also account for the presence of an elastic crust, perhaps penetrated by a neutron superfluid, and include dissipative processes such as mutual friction and β-reactions between the two fluids. Another issue that needs to be studied in detail is the potential gravitational-radiation instability of the various modes, and a suitable adaptation of the Chandrasekhar–Friedman–Schutz (CFS) instability criterion (Chandrasekhar 1970; Friedman & Schutz 1978) to non-corotating backgrounds. This should also help shed light on the two-stream instability, the true physical relevance of which is difficult to assess at the present time.

ACKNOWLEDGMENTS

We thank L. Valdettaro and M. Rieutord for allowing us to use their LSB code, and we further thank B. Dintrans and M. Rieutord for valuable discussions and help with the numerics. RP and NA acknowledge support from the EU Programme 'Improving the Human Research Potential and the Socio-Economic Knowledge Base' (Research Training Network Contract HPRN-CT-2000-00137). GLC gratefully acknowledges support from NSF grant PHYS-0140138. NA is grateful for generous support from a Philip Leverhulme Prize fellowship.

REFERENCES

Alpar M., Langer S., Sauls J., 1984, ApJ, 282, 533
Andersson N., 1998, ApJ, 502, 708
Andersson N., Comer G., 2001, MNRAS, 328, 1129
Andersson N., Comer G., Langlois D., 2002, Phys. Rev. D, 66, 104002
Andersson N., Comer G., Prix R., 2003, Phys. Rev. Lett., 90, 091101
Batchelor G. K., 1953, Q. J. R. Meteorol. Soc., 79, 224
Bryan G., 1889, Phil. Trans. R. Soc. Lond., 180, 187
Carter B., 1989, in Anile A., Choquet-Bruhat M., eds, Lecture Notes in Mathematics, Vol. 1385, Relativistic Fluid Dynamics (Noto, 1987). Springer-Verlag, Heidelberg, p. 1
Carter B., Khalatnikov I., 1992, Ann. Phys. NY, 219, 243
Carter B., Langlois D., 1998, Nucl. Phys. B, 531, 478
Chandrasekhar S., 1970, Phys. Rev. Lett., 24, 611
Comer G., 2002, Found. Phys., 32, 1903
Dintrans B., Rieutord M., 2001, MNRAS, 324, 635
Friedman J. L., Morsink S. M., 1998, ApJ, 502, 714
Friedman J. L., Schutz B. F., 1978, ApJ, 222, 281
Langlois D., Sedrakian D. M., Carter B., 1998, MNRAS, 297, 1189
Lee U., 1995, A&A, 303, 515
Lee U., Yoshida S., 2003, ApJ, 586, 403
Lindblom L., Mendell G., 1994, ApJ, 421, 689
Lindblom L., Mendell G., 2000, Phys. Rev. D, 61, 104003
Lockitch K. H., Friedman J. L., 1999, ApJ, 521, 764
Ogura Y., Phillips N. A., 1962, J. Atmos. Sci., 19, 173
Pierce J., 1974, Almost All About Waves. MIT Press, Cambridge, MA
Prix R., 2003, Phys. Rev. D, in press
Prix R., 2004, Phys. Rev. D, submitted
Prix R., Rieutord M., 2002, A&A, 393, 949
Prix R., Comer G., Andersson N., 2002, A&A, 381, 178
Rieutord M., Dintrans B., 2002, MNRAS, 337, 1087
Sedrakian A., Wasserman I., 2000, Phys. Rev. D, 63, 024016
Villain L., Bonazzola S., 2002, Phys. Rev. D, 66, 123001
Yoshida S., Lee U., 2003a, MNRAS, 344, 207
Yoshida S., Lee U., 2003b, Phys. Rev. D, 67, 124019

APPENDIX A: THE ANELASTIC APPROXIMATION

The anelastic approximation was first introduced in atmospheric physics (Batchelor 1953; Ogura & Phillips 1962) and has since also been widely used in the study of stellar oscillations and convection. A more detailed analysis of the quality and justification of this approximation in the case of g modes can be found in Dintrans & Rieutord (2001) and Rieutord & Dintrans (2002), and it has also been used recently in the study of inertial modes (Villain & Bonazzola 2002). The anelastic approximation applies for modes with frequencies which are small compared to the inverse of the sound crossing time of the star, which characterizes the lowest-order p-mode frequency. High-frequency modes such as p modes are effectively 'filtered out' by this approximation, so that only low-frequency modes such as inertial modes or g modes remain. We will now briefly sketch how this approximation works in the study of inertial modes of a barotropic star. We start from the linear perturbation equations for a uniformly rotating barotrope, assuming an eigenmode solution of the form $\mathrm{e}^{\mathrm{i}(\omega t+m\varphi)}$, which yields

$$\mathrm{i}(\omega + m\Omega)\delta n + \nabla\cdot(n\delta\boldsymbol{v}) = 0, \tag{A1}$$

$$\mathrm{i}(\omega + m\Omega)\delta\boldsymbol{v} + 2\Omega\hat{\boldsymbol{z}}\times\delta\boldsymbol{v} + \nabla(\delta\widetilde{\mu} + \delta\phi) = 0. \tag{A2}$$

We choose an average sound speed c_0 as the natural velocity scale, and the stellar radius R as length-scale, which implies the sound crossing time R/c_0 as the natural time-scale. Therefore the dimensionless mode frequency is

$$\widehat{\omega} \equiv \frac{\omega}{c_0/R}. \tag{A3}$$

Inertial modes have the property that their frequencies are of the order of Ω, so we introduce

$$\zeta \equiv \frac{\Omega}{\omega} = \mathcal{O}(1). \tag{A4}$$

From the relation between pressure perturbations and density perturbations we obtain

$$\delta P = \rho\delta\widetilde{\mu} = c_{\mathrm{s}}^2\delta\rho, \qquad \Longrightarrow \qquad n\delta\widetilde{\mu} = c_{\mathrm{s}}^2\delta n. \tag{A5}$$

We write the local sound speed $c_{\mathrm{s}}(r)$ as

$$c_{\mathrm{s}}(r) = \lambda(r)c_0, \tag{A6}$$

where $\lambda(r)$ is a function of order unity in the bulk of the star, but which usually vanishes at the stellar surface. As $\delta\widetilde{\mu}$ has the dimensions of a velocity squared, the relation (A5) takes the following form in natural units:

$$n\delta\widetilde{\mu} = \lambda^2(r)\delta n. \tag{A7}$$

So, $\delta\widetilde{\mu}$ and δn are seen to be of the same order except close to the surface if $\lambda \to 0$. In this system of units, the perturbation equations can now be written as

$$\widehat{\omega}\lambda^{-2}\mathrm{i}(1 + m\zeta)n\delta\widetilde{\mu} + \nabla\cdot(n\delta\boldsymbol{v}) = 0, \tag{A8}$$

$$\widehat{\omega}[\mathrm{i}(1 + m\zeta)\delta\boldsymbol{v} + 2\zeta\hat{\boldsymbol{z}}\times\delta\boldsymbol{v}] + \nabla(\delta\widetilde{\mu} + \delta\phi) = 0. \tag{A9}$$

We restrict ourselves to modes that have low frequencies compared to the sound crossing frequency c_0/R, so we assume

$$\widehat{\omega} \ll 1. \tag{A10}$$

It is straightforward to see from equation (A9) that

$$\delta\widetilde{\mu} = \mathcal{O}(\widehat{\omega}), \tag{A11}$$

and therefore equation (A8) yields

$$\nabla \cdot (n\delta\boldsymbol{v}) = \mathcal{O}(\widehat{\omega}^2\lambda^{-2}). \tag{A12}$$

In the bulk of the star, where $\lambda \sim \mathcal{O}(1)$, we can therefore neglect the density variation δn in the conservation equation, leading to an error of order $\mathcal{O}(\widehat{\omega}^2)$. However, in the boundary layer characterized by $\lambda \sim \mathcal{O}(\widehat{\omega})$, i.e. in the region where the local sound speed is of order $c_{\rm s} \sim \omega R$, the error of neglecting the compressibility of the matter becomes large. Nevertheless, the overall quality of the approximation is generally very good (see Dintrans & Rieutord 2001), provided this surface boundary layer is sufficiently thin, but we might expect the surface boundary conditions to be modified. This is indeed the case, as equation (A12) now entails the regularity condition $\delta v^r|_{r=R} = 0$ for stellar modes with $\rho \to 0$ at the surface. Therefore, the surface displacement is necessarily zero in the anelastic approximation, which filters out any surface waves. Another consequence of this approximation is seen by taking the curl of equation (A9), which effectively eliminates the potentials $\delta\widetilde{\mu}$ and $\delta\phi$ from the system of equations. The velocity perturbation is therefore independent of the pressure perturbation and gravitational perturbation, which can both be determined a posteriori from the solution and the remaining component of the Euler equation. The eigenmode solution is therefore independent of all potential perturbations, $\delta\phi$, δP (or equivalently $\delta\widetilde{\mu}$). Although these perturbations were not assumed to be zero, they are now 'slaved' to the velocity perturbation.

APPENDIX B: THE EXPLICIT OSCILLATION EQUATIONS

The general system of equations (44)–(47) for the eigenmode problem together with the definitions in Section 6 can be written in the explicit form

$$r W_{\rm n}^{l'} + \left(1 + r\frac{\rho_{\rm n}'}{\rho_{\rm n}}\right) W_{\rm n}^l - l(l+1)V_{\rm n}^l = 0, \tag{B1}$$

$$r W_{\rm p}^{l'} + \left(1 + r\frac{\rho_{\rm p}'}{\rho_{\rm p}}\right) W_{\rm p}^l - l(l+1)V_{\rm p}^l = 0, \tag{B2}$$

$$\begin{aligned}&(l-1)Q_l U_{\rm n}^{l-1} - (l+2)Q_{l+1}U_{\rm n}^{l+1} + mV_{\rm n}^l \\ &\quad - (1-\varepsilon_{\rm n})\nu_{\rm n} m\mathcal{R}W_{\rm n}^l - \varepsilon_{\rm n}\nu_{\rm n} m\mathcal{R}W_{\rm p}^l + r\widehat{\psi}_{\rm n}^{l'} \\ &\quad = \kappa_0\left[(1-\varepsilon_{\rm n})\nu_{\rm n}W_{\rm n}^l + \varepsilon_{\rm n}\nu_{\rm n}W_{\rm p}^l\right],\end{aligned} \tag{B3}$$

$$\begin{aligned}&(l-1)Q_l U_{\rm p}^{l-1} - (l+2)Q_{l+1}U_{\rm p}^{l+1} + mV_{\rm p}^l + r\widehat{\psi}_{\rm p}^{l'} \\ &\quad = \kappa_0\left[(1-\varepsilon_{\rm p})\nu_{\rm p}W_{\rm p}^l + \varepsilon_{\rm p}\nu_{\rm p}W_{\rm n}^l\right],\end{aligned} \tag{B4}$$

$$\begin{aligned}&(l^2-1)Q_l U_{\rm n}^{l-1} + l(l+2)Q_{l+1}U_{\rm n}^{l+1} \\ &\quad + \{m - l(l+1)(1-\varepsilon_{\rm n})\nu_{\rm n}m\mathcal{R}\}\,V_{\rm n}^l \\ &\quad - l(l+1)\varepsilon_{\rm n}\nu_{\rm n}m\mathcal{R}V_{\rm p}^l + mW_{\rm n}^l + l(l+1)\widehat{\psi}_{\rm n}^l \\ &\quad = \kappa_0\left[l(l+1)(1-\varepsilon_{\rm n})\nu_{\rm n}V_{\rm n}^l + l(l+1)\varepsilon_{\rm n}\nu_{\rm n}V_{\rm p}^l\right],\end{aligned} \tag{B5}$$

$$\begin{aligned}&(l^2-1)Q_l U_{\rm p}^{l-1} + l(l+2)Q_{l+1}U_{\rm p}^{l+1} \\ &\quad + mV_{\rm p}^l + mW_{\rm p}^l + l(l+1)\widehat{\psi}_{\rm p}^l \\ &\quad = \kappa_0\left[l(l+1)(1-\varepsilon_{\rm p})\nu_{\rm p}V_{\rm p}^l + l(l+1)\varepsilon_{\rm p}\nu_{\rm p}V_{\rm n}^l\right],\end{aligned} \tag{B6}$$

$$\begin{aligned}&\{m - l(l+1)(1-\varepsilon_{\rm n})\nu_{\rm n}m\mathcal{R}\}U_{\rm n}^l \\ &\quad - l(l+1)\varepsilon_{\rm n}\nu_{\rm n}m\mathcal{R}U_{\rm p}^l \\ &\quad + (l^2-1)Q_l V_{\rm n}^{l-1} + l(l+2)Q_{l+1}V_{\rm n}^{l+1} \\ &\quad - (l+1)Q_l W_{\rm n}^{l-1} + lQ_{l+1}W_{\rm n}^{l+1} \\ &\quad = \kappa_0\left[l(l+1)(1-\varepsilon_{\rm n})\nu_{\rm n}U_{\rm n}^l + l(l+1)\varepsilon_{\rm n}\nu_{\rm n}U_{\rm p}^l\right],\end{aligned} \tag{B7}$$

$$\begin{aligned}&mU_{\rm p}^l + (l^2-1)Q_l V_{\rm p}^{l-1} + l(l+2)Q_{l+1}V_{\rm p}^{l+1} \\ &\quad - (l+1)Q_l W_{\rm p}^{l-1} + lQ_{l+1}W_{\rm p}^{l+1} \\ &\quad = \kappa_0\left[l(l+1)(1-\varepsilon_{\rm p})\nu_{\rm p}U_{\rm p}^l + l(l+1)\varepsilon_{\rm p}\nu_{\rm p}U_{\rm n}^l\right].\end{aligned} \tag{B8}$$

This paper has been typeset from a TEX/LATEX file prepared by the author.